

1 **Hyperplex PCR enables the next-generation of wastewater-**
2 **based surveillance systems: long-term SARS-CoV-2 variant**
3 **surveillance in Sweden as a case study**

4 *Ruben R. G. Soares*^{d*}; *Javier Edo Varg*^a; *Attila Szabó*^{a, c}; *Margarita Psallida*^d;
5 *Paweł Olszewski*^d; *Danai V. Nikou*^d; *Umear Naseem*^d; *Maja Malmberg*^b; *Anna J. Székely*^{a*}

6 ^a Department of Aquatic Sciences and Assessment, Swedish University of Agricultural
7 Sciences, Box 7050, 75007, Uppsala, Sweden

8 ^b Department of Animal Biosciences, Swedish University of Agricultural Sciences, Box
9 7023, 750 07 Uppsala, Sweden

10 ^c Institute of Aquatic Ecology, HUN-REN Centre for Ecological Research, Karolina str.
11 29., H- 1113 Budapest, Hungary

12 ^d Aplex Bio AB, Nobels väg 16, 171 65, Solna, Sweden

13

14 * Contact authors:

15 Ruben R.G. Soares; Nobels väg 16, Solna, Sweden; ruben@aplex.bio

16 Anna J. Székely; Lennart Hjelms väg 9, Uppsala, Sweden; anna.szekely@slu.se

17

18 **Abstract**

19 Wastewater-based epidemiology aims at measuring pathogens in wastewater as a
20 means of deriving unbiased epidemiological information at a population scale, ranging
21 from buildings and aircrafts to entire cities or countries. After gaining significant
22 mainstream attention during the SARS-CoV-2 pandemic, the field holds significant
23 promise as a continuous monitoring and early warning system tracking emerging viral
24 variants or new pathogens with pandemic potential.

25 To expand the current toolbox of analytical techniques for wastewater analysis,
26 we explored the use of Hyperplex PCR (hpPCR) to analyse SARS-CoV-2 mutations in
27 wastewater samples collected weekly in up to 22 sites across Sweden between October
28 2022 and December 2023. Approximately 900 samples were tested using a dynamic
29 probe panel with a multiplexity ranging from 10- to 18-plex, continuously adapted within
30 1-2 weeks to quantify relevant mutations of concern over time. The panel simultaneously
31 covered deletions, single nucleotide substitutions, as well as variable regions resorting to
32 probe degeneracy. By analysing all samples in parallel resorting to gold standard methods
33 including qPCR and two different NGS technologies, the performance of hpPCR is herein
34 shown to bridge the gap between these methods by providing (1) systematic single
35 nucleotide sensitivity with a simple probe design, (2) high multiplexity without panel re-
36 optimization requirements and (3) 4-5-week earlier mutation detection compared to NGS
37 with excellent quantitative linearity and a good correlation for mutation frequency
38 ($r=0.88$). Based on the demonstrated performance, the authors propose the combined use
39 of NGS and hpPCR for routine discovery and high-frequency monitoring of key
40 pathogens/variants as a potential alternative to the current analysis paradigm.

41

42

43 **Keywords:** hpPCR; wastewater-based epidemiology; mutations; monitoring; padlock
44 probes; rolling circle amplification

45

46

47 **1. Introduction**

48 Wastewater-based epidemiology (WBE), although being an 80-year-old concept, only
49 reached the lab bench in the early 2000's and recently catapulted to mainstream attention
50 during the 2020 SARS-CoV-2 pandemic [1] As the name implies, the field aims at
51 analysing wastewater samples for the presence and quantity of infectious agents to derive
52 epidemiological information at population level. There is currently an increasing body of
53 evidence showing the potential of this approach as a reliable and intrinsically unbiased
54 proxy of total cases in each population, thus easing the economic and logistical burden of
55 mass population testing [2], [3]. The latter becomes particularly relevant to enable
56 successful implementation of pandemic preparedness systems for national level routine
57 monitoring of circulating and emerging pathogens [4]. This approach has been tested both
58 at city/municipality-level and at smaller scales, such as buildings (e.g. office spaces and
59 airports) and airplanes [5], ultimately allowing to trace the origin of novel mutations to
60 specific sites [6]. All these serve as key examples where a developed WBE toolbox can
61 serve as a key resource in pandemic preparedness by enabling more efficient and
62 information-driven containment policies. However, there are still multiple barriers
63 towards reaching such degree of maturity, ranging from (1) detecting highly diluted and
64 potentially degraded RNA in the PCR inhibitor-rich wastewater matrix, to (2) the
65 challenges in implementing adequate sampling protocols, transport logistics and assay
66 controls to ensure that the measured target concentrations adequately represent the
67 population and can be reliably compared between different sampling sites and sampling
68 times [1]. To address these challenges, sensitive, specific, mass deployable, scalable,
69 rapid, and cost-efficient methods allowing high-frequency sampling are in demand to
70 gather and share high volumes of data required to consolidate WBE as a routine
71 surveillance tool.

72 The current analytical toolbox to measure SARS-CoV-2 RNA in wastewater comprises a
73 first concentration and extraction-step, aiming at maximizing RNA titers while reducing
74 the concentration of potential inhibitors [7]. Then, targeted, or non-targeted analytical
75 methods are used for qualitative or quantitative analysis. Targeted methods include
76 quantitative PCR (qPCR) and digital PCR (dPCR) and non-targeted analysis is typically
77 done using next generation sequencing (NGS). Reverse transcription-qPCR (RT-qPCR)
78 is currently the most cost-effective option and provides high sensitivity combined with a
79 wide dynamic range, being the standard workhorse for wastewater monitoring,

80 particularly when measuring total SARS-CoV-2 virus titers targeting conserved
81 sequences [8]. On the other hand, despite increased running costs [9], there is an
82 increasing shift towards ddPCR based on substantial [10], [11], albeit not undisputed [9]
83 evidence of higher sensitivity and resistance to inhibition. However, despite significant
84 efforts to apply both RT-qPCR [12], [13], [14], [15] and dPCR [16], [17], [18], [19] for
85 SARS-CoV-2 variant surveillance using hydrolysis probes, protocol optimization to
86 target point mutations typically requires extensive adjustment of annealing temperatures
87 to avoid false-positive detections [12]. Additionally, locked nucleic acids (LNA) might
88 have to be introduced into the probe sequence to increase specificity [15], and background
89 signals often interfere with the results particularly for high concentrations of off-target
90 sequences (e.g. wild-type sequence) [9]. Furthermore, both methods are limited in the
91 degree of multiplexity per sample, often capped at less than 6 targets per sample which is
92 suboptimal for a broad-scope variant analysis. All these factors cause delays and practical
93 barriers in implementing fit-for-purpose assays for emerging variants, consequently
94 forcing researchers to turn towards targeted NGS [20], [21], [22] despite the substantially
95 higher consumable and labour costs. To address the specificity and multiplexity
96 limitations of RT-qPCR and dPCR, while avoiding the increased costs and complexity of
97 NGS, Hyperplex PCR (hpPCR) integrates RT-PCR, padlock probes (PLPs), rolling circle
98 amplification (RCA) [23] and optically encoded probes [24]. This approach ensures
99 robust single-nucleotide specificity combined with massive multiplexity of more than 100
100 targets per sample through post-amplification optical fluorescence imaging.

101

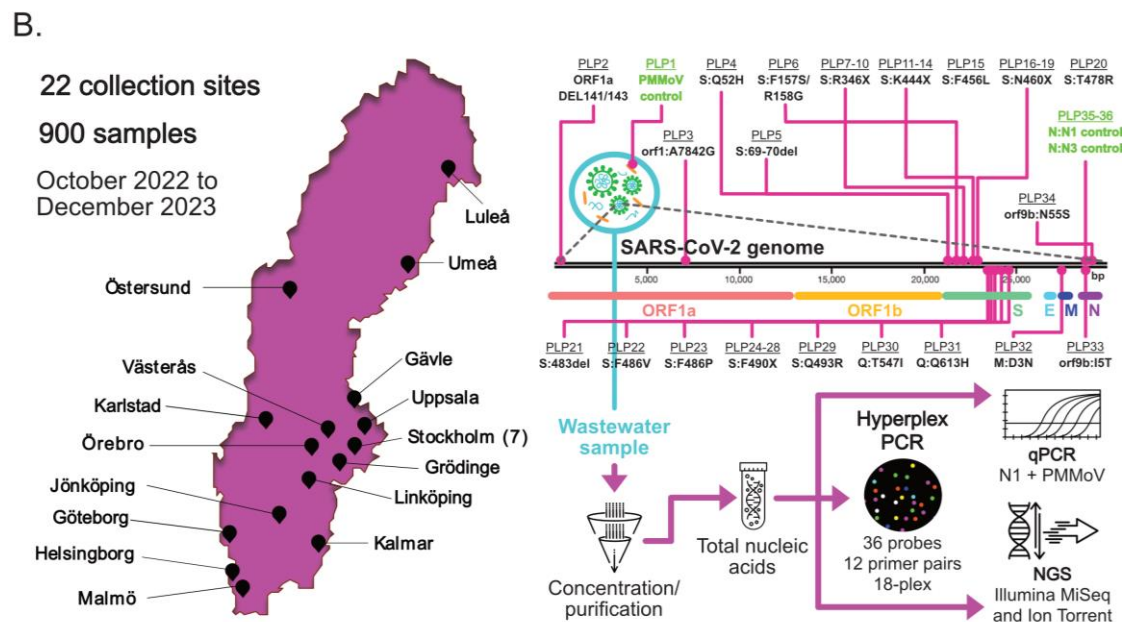
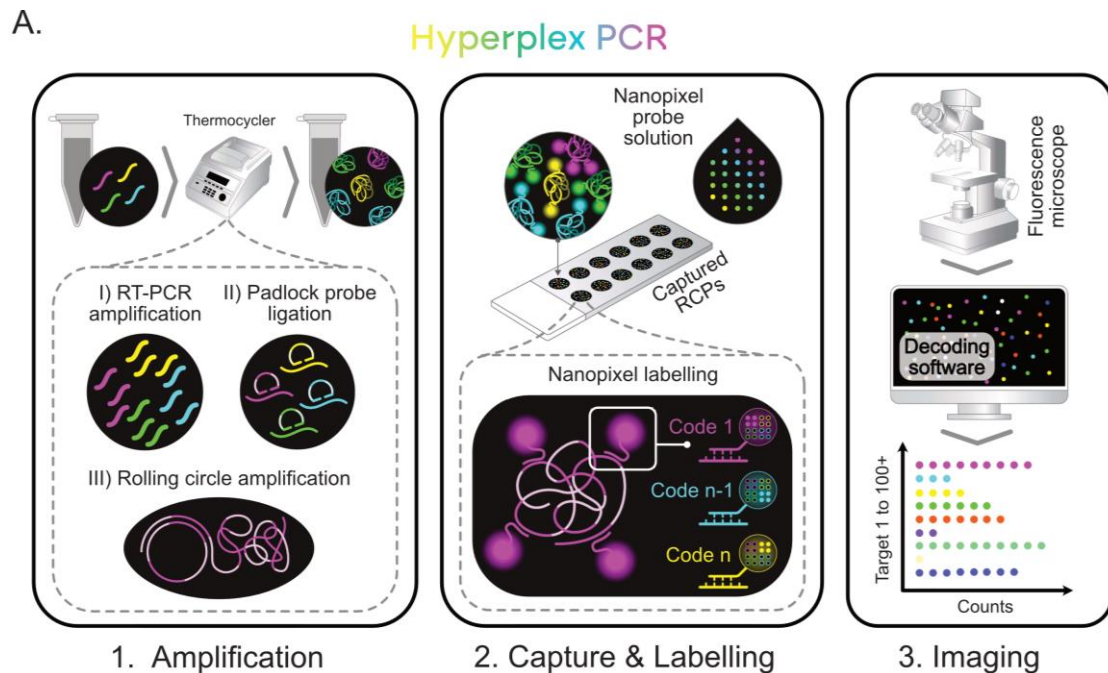
102 **2. Results and Discussion**

103 **2.1. Methodology and study overview**

104 The main goal of this study was to evaluate the performance of Hyperplex PCR (hpPCR)
105 in the context of multiplex targeted quantification of SARS-CoV-2 mutations of concern
106 in wastewater samples. The workflow of Hyperplex PCR is schematized in Figure 1-A
107 and comprises 3 main steps. The first step includes a 1-step RT-PCR amplification of the
108 target regions of interest, padlock probe (PLP) ligation to the target mutations and rolling
109 circle amplification of the ligated probes. The ligation of the panel of PLPs was performed
110 after dilution of the PCR amplicons, allowing for archiving of PCR amplicons and re-
111 probing of mutations within the same amplicons. Performing the probing with a ligation
112 reaction instead of typical hybridization-based hydrolysis probes (e.g. TaqMan probes or

113 molecular beacons), particularly when using thermostable ligases ensures systematic and
114 virtually optimization-free single nucleotide specificity under optimized conditions [25].
115 Each padlock probe contains a proprietary barcode in the backbone (sequence between
116 the left and right arms) resulting in a total length of 96 bp for each probe. The subsequent
117 RCA step generates amplification products of about 1 μm in diameter containing about
118 1-2 thousand copies of the barcode sequence. In the second step, the rolling circle
119 amplification products (RCPs) are captured on a surface and each barcode will be
120 specifically recognized by Nanopixel probes having a unique optical code corresponding
121 to each target barcode of the PLPs. In the final third step, the surface is imaged with
122 fluorescence microscopy and RCPs of each specific optical barcode are counted and
123 normalized to an internal RCP reference to neutralize variation in capture efficiency.
124 Figure 1-B illustrates the collection sites, probe design map within the SARS-CoV-2
125 genome, and sample analysis logistics. From October 2022 to December 2023,
126 approximately 900 wastewater samples were collected weekly from up to 22 wastewater
127 treatment plants across Sweden, including 6 located in Stockholm municipality (Table
128 S7). During the analysis period a total of 36 PLPs were designed targeting 12 RT-PCR
129 amplified regions of the SARS-CoV-2 genome. Three probes were dedicated to internal
130 control targets, namely PMMoV as a marker of human fecal material and N1 (up to
131 w15/2023) or N3 (from w16/2023) as conserved SARS-CoV-2 genes. The remaining 33
132 probes were designed to target key mutations characteristic of emerging SARS-CoV-2
133 variants of concern. Among this probe set, (1) single nucleotide substitutions, (2)
134 deletions and (3) pooled mutation profiling were achieved simultaneously with different
135 probe designs. PLPs for single nucleotide substitutions were preferably designed with the
136 mutation placed on the 3' end, PLPs for deletions were designed with the extremes of the
137 deleted region complementary to each probe arm and pooled mutation profiling
138 (designated as "X" amino acid substitutions in Figure 1-B) was achieved using degenerate
139 bases and common barcodes (corresponding to the same Nanopixel probe) in the PLP
140 backbone. The PCR primers and PLPs included in the analysis were modified throughout
141 the study (Methods section 4.4.1), from initially 10-plex to an 18-plex panel by Summer
142 2023 upon the emergence of the BA.2.86 variant.
143 Since one of the key objectives of the study was to evaluate if Hyperplex PCR could
144 improve WBE analysis compared to current methodologies, in particular non-targeted
145 approaches, all collected samples were split after extraction and measured in parallel
146 using conventional qPCR and one of two NGS methods, namely optical- (Illumina) and

147 semiconductor-based (Ion Torrent) sequencing. (Ion Torrent: w40/2022-w21/2023 and
 148 w35-36/2023, and Illumina: w22-34/2023 and w37-52/2023). The following subsections
 149 explore the output of Hyperplex PCR compared to qPCR, and NGS, as well as published
 150 clinical data to validate its relevance in the context of WBE and future pandemic
 151 preparedness.



152
 153 **Figure 1:** Hyperplex PCR workflow and overview of wastewater collection and analysis
 154 approach. **A-** Workflow of Hyperplex PCR comprising 3 main analytical steps: (1) amplification
 155 of extracted nucleic acids by reverse transcription PCR (RT-PCR), followed by padlock probe
 156 (PLP) ligation and re-amplification of the PCR amplicons into rolling circle amplification
 157 products (RCPs); (2) Capture of the RCPs on a solid phase with a SLAS format and subsequent

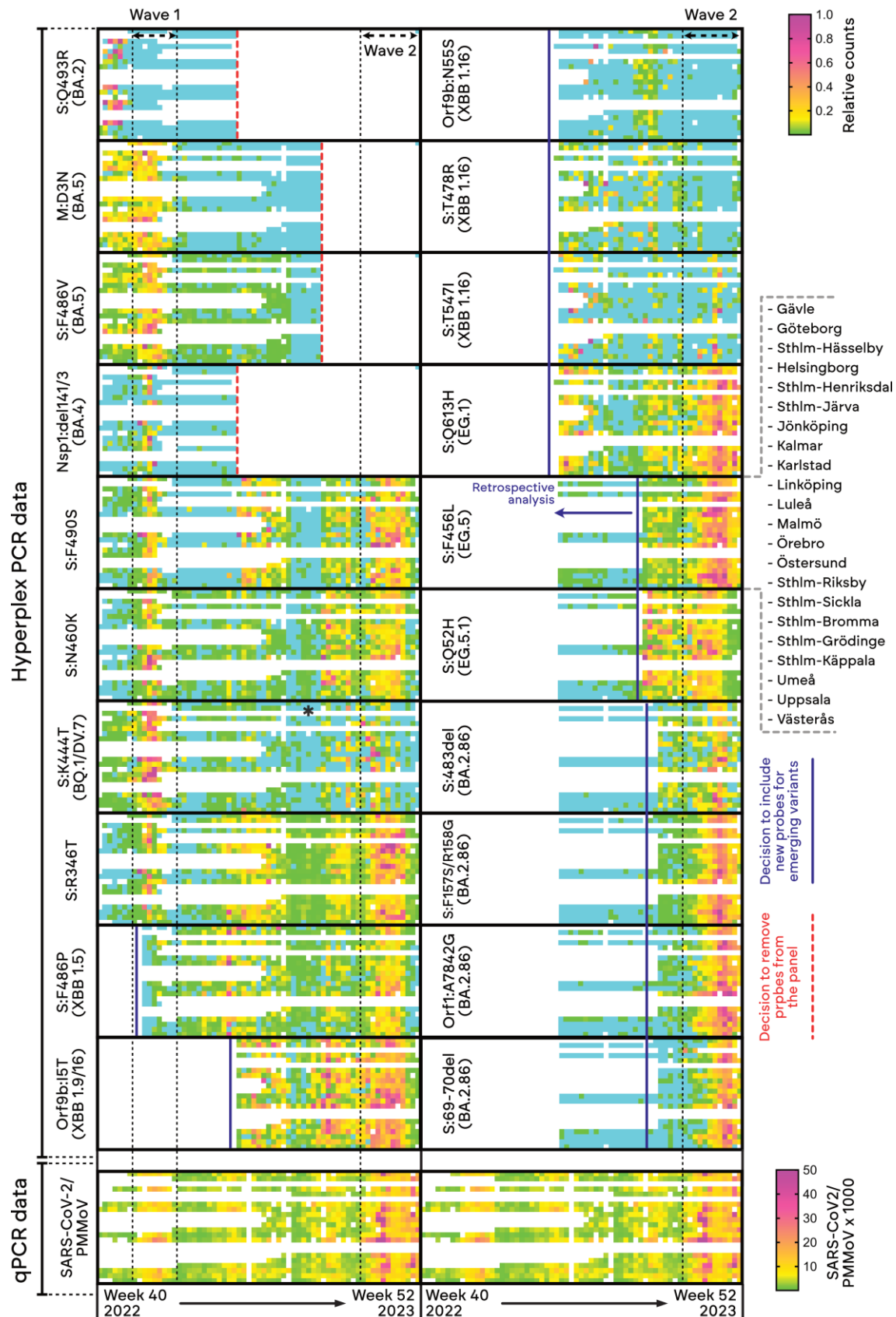
158 hybridization to Nanopixel probes and; (3) Imaging of the Nanopixel-probed RCPs using an
159 epifluorescence microscope, followed by decoding of the Nanopixel optical probes using a
160 proprietary image analysis tool from APLEX Bio which converts the image into RCP counts per
161 PLP target sequence. **B-** Design of long-term study and analytical approach using Hyperplex PCR,
162 qPCR, Illumina and Ion Torrent in parallel for each extracted sample. For Hyperplex PCR, a total
163 of 12 PCR primer pairs and 36 PLPs were designed spanning the entire genome of SARS-CoV-
164 2. To adapt to outcompeted and emerging viral variants over time, not all probes were used
165 simultaneously and up to 18-plex target analysis was performed. The “X” in the amino-acid
166 substitution nomenclature refers to multiple mutations being covered by a set of degenerate PLPs
167 encoded by the same Nanopixel probe.

168

169 **2.2. Hyperplex PCR allows multiplexed relative quantification of at least 18** 170 **mutations of concern per assay with rapid panel customization**

171 The qPCR and hpPCR results obtained for all tested samples are summarized as heat
172 maps in Figure 2. For qPCR the color coding corresponds to concentration of N1 copies
173 normalized to PMMoV. For hpPCR, the results are expressed as relative counts, meaning
174 the absolute signal of the assay for a specific target (according to methods section 4.4.3)
175 normalized to the highest absolute signal measured for that same specific target within
176 the entire dataset. This relative normalization was applied since the efficiency of PCR
177 amplification was not calibrated between targets, hence making the absolute counts not
178 comparable between different mutations, particularly those targeting sequences in
179 different PCR amplicons, but comparable between different time-points (x-axis) and
180 collection sites (y-axis). While the assay could be designed to provide absolute
181 quantification for each mutation with appropriate internal controls and/or calibration
182 curves, the original aim of the application of the hpPCR method was to complement the
183 ongoing viral quantification efforts with variant composition assessment. Overall, the
184 results in Figure 2 highlight the expanded dataset obtained using hpPCR compared to
185 qPCR, allowing the discrimination of trends for several key mutations of concern
186 according to the recommendations of health authorities at a given time point. Since PLPs
187 ensure reliable single nucleotide specificity with minimal requirements of assay
188 optimization, the targets in the panel can be adapted on demand by including new
189 primers/probes for emerging mutations of concern (solid vertical lines in Figure 2) or
190 excluding primers/probes targeting outcompeted mutations (dashed vertical lines in
191 Figure 2). Upon emergence of a new mutation of interest, the delay to implement a new
192 probe was less than 2 weeks including design (< 1 day), oligo procurement (5-10 days),

193 and PCR primer/PLP mix formulation (< 1 day). Two main waves of infection were
194 observed throughout the testing period, during the winter season of 2022 and
195 autumn/winter season of 2023. During these periods of increased SARS-CoV-2 viral
196 titers in wastewater samples, already prevalent and particularly emerging mutations were
197 also found to peak during those periods, namely S:346X (XBB, BA.2.75), S:K444X
198 (BQ.1), S:N460X (BQ.1, BA.2.75, XBB) and S:F490S (BJ.1, XBB.1) during the first
199 wave and BA.2.86 mutations (S:483del, S:F157S/R158G, Orf1:A7842G and S:69-70del)
200 during the second wave. Overall, the trends measured for each mutation provided an
201 excellent correlation with trends observed for clinical cases during periods of active
202 clinical monitoring (Figure S1, where the clinical cases for each mutation were estimated
203 using the CoV-Spectrum Portal [26] and the total SARS-CoV-2 incidence published by
204 The Public Health Agency of Sweden - data accessed on March 2023) and successfully
205 allowed the surveillance of re-emerging mutations such as S:K444T from the first clinical
206 cases of DV.7.1 in w30/2023 (asterisk in Figure 2) until virtually zero incidence by
207 w52/2023. Clinical incidence of DV.7.1 was obtained from the CoV-Spectrum portal [26]
208 accessed in March 2024. Considering that upon the decision to implement probes
209 targeting S:F456L, S:Q52H and BA.86 mutations, positive signals were found in most of
210 the tested cities, a retrospective analysis was performed for the 8 sites covering more than
211 100.000 people in the catchment area back to w16/2023 to test the early detection of these
212 variants. The results of this retrospective analysis are described below in section 2.3.



213

214

215

216

Figure 2: Heatmap plot summarizing the Hyperplex PCR and qPCR results obtained for all tested samples between October 2022 and December 2023 with a frequency of one sample per week for each collection site. qPCR targeted SARS-CoV-2 using the N1 assay until w29/2023 and SCV2

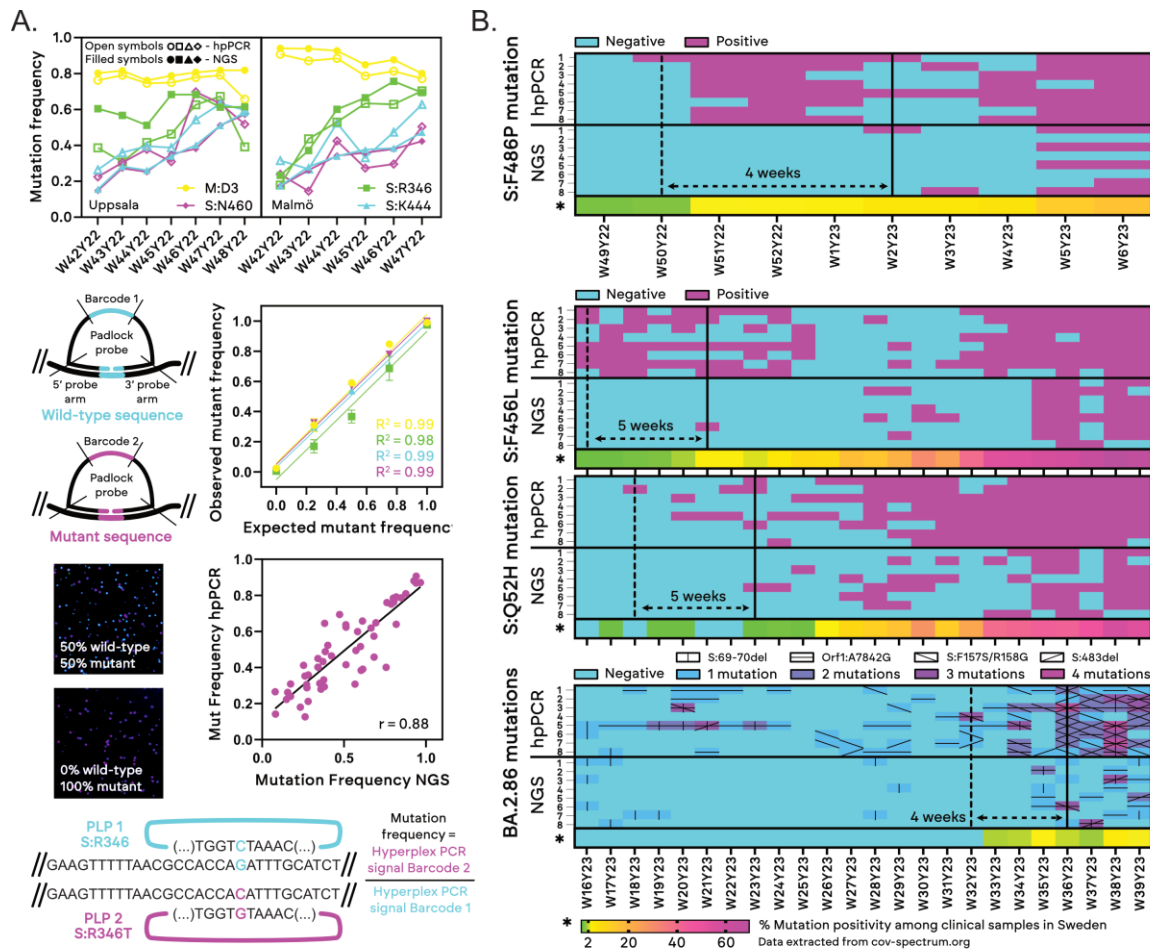
217 onwards. For each target sequence, columns correspond to weekly measurements and rows to
218 each of the 22 collection sites (Table S7). For Hyperplex PCR relative counts refer to signal
219 obtained for each target sequence normalized to the maximum intensity measured for each target
220 among all samples. The blue color code refers to signals below the detection threshold. Variants
221 indicated for each mutation refer to the most prevalent variant associated to the mutation at the
222 time the probes were included in the panel. The asterisk in the S:K444T panel refers to the
223 identification of the first clinical cases of DV.7.1 in Sweden. The qPCR data is duplicated below
224 each column of 10 hpPCR targets for visualization purposes.

225

226 **2.3. Hyperplex PCR provides mutation frequency quantification comparable to** 227 **NGS with significantly higher sensitivity**

228 Expanding on the quantitative capabilities of hpPCR beyond the relative quantification
229 of target mutations over time in multiple sites, additional probes targeting the wild-type
230 sequence of specific target mutations were added to evaluate the quantification of
231 mutation frequency (MF). By quantifying MF it becomes possible to compare the
232 prevalence of different target mutations by having the total virus (Wt plus Mut sequences)
233 as internal control. In this case, two gold standard NGS methods typically used for
234 wastewater analysis, namely Illumina and Ion Torrent were used to benchmark the MF
235 output of the hpPCR assay focusing on samples collected around the period of wave 1.
236 The MF quantification concept and summary of results are shown in Figure 3-A.
237 According to the example schematics and imaging example of 2-plex results for mutation
238 S:R346T, two uniquely barcoded PLPs are used to target the wild-type (G22599) or
239 mutated sequences (G22599C). The plots highlight the following three key observations.
240 (1) A good correlation of hpPCR and NGS when measuring MF over time for each of the
241 four target mutations was observed, here tested for 2 different major populational centers,
242 namely Uppsala and Malmö covering 191 000 and 356 000 people in the catchment area,
243 respectively. Importantly, both measurements agree with the proportion of SARS-CoV-2
244 clinical samples found with these mutations in Sweden during this period (Figure S2). (2)
245 Spiking known mixtures of synthetic amplicons containing each of the target mutations,
246 hpPCR provides an excellent linearity ($R^2=0.99$) and agreement between expected and
247 observed MF values. (3) Pooling all data obtained for both Uppsala and Malmö samples
248 between w42/2022 and w48/2022, a Pearson correlation coefficient of 0.88 was obtained
249 between the MF output of hpPCR and NGS. Overall, these observations indicate that
250 hpPCR can serve as a viable alternative to NGS for the targeted quantification of point

251 mutation frequency in wastewater. Furthermore, hpPCR was further compared with NGS
252 concerning sensitivity to allow early detection of emerging mutations of concern
253 according to the results in Figure 3-B. Using hpPCR it was systematically possible to
254 detect positivity for emerging mutations 4 to 5 weeks earlier compared to NGS for 3 key
255 mutations characteristic of highly relevant VOCs, namely XBB 1.5 and EG.5 and a set of
256 mutations characteristic of BA.2.86. Remarkably, the readout using hpPCR provided a
257 superior correlation with clinical incidence and early detection when mutation specific
258 incidence represented less than 2% of the total SARS-CoV-2 clinical cases. In the case of
259 BA.2.86, which had several differentiating characteristic mutations relative to other
260 coexisting XBB and BA.5-descendant variants, based on early sequencing data from
261 Swedish patients, only a small subset of 4 mutations were selected for monitoring using
262 hpPCR. Nevertheless, even considering all BA.2.86 characteristic mutations measured
263 using NGS, hpPCR still provided a 3-week earlier detection targeting 4 mutations within
264 the same list of BA2.86 characteristic mutations considered for NGS positivity (Figure
265 S3, Table S6). Interestingly, two samples with at least 3 key mutations of BA.2.86 were
266 found in w20 and w21, in line with the results of NGS considering all BA.2.86 mutations,
267 albeit for different targets and sites (Figure S3, Table S6). Ultimately, combining the
268 possibility of rapidly implementing probes with NGS-grade specificity but having a
269 sensitivity significantly higher than NGS, hpPCR intrinsically enables earlier detection
270 of targets than currently available targeted and non-targeted gold standard methods.



271

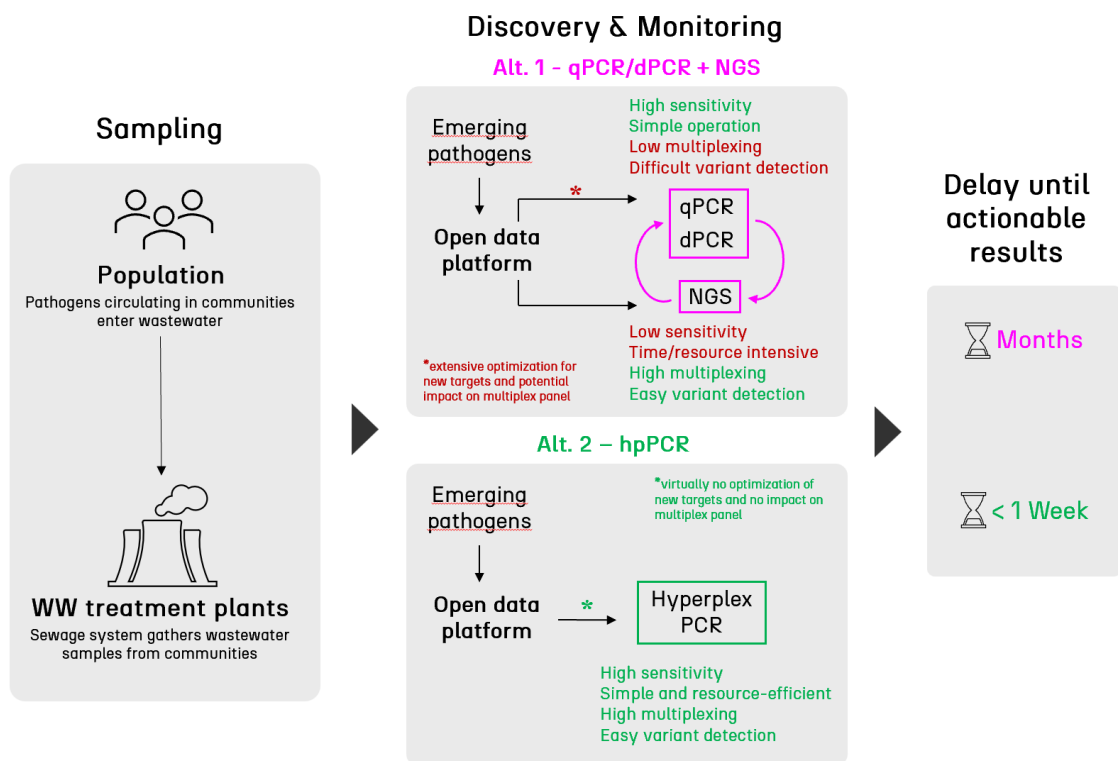
272 **Figure 3:** Benchmarking of quantitative performance (A) and sensitivity (B) of Hyperplex PCR
 273 against next-generation sequencing (NGS). **A-** Conceptual schematic and demonstration of
 274 Hyperplex PCR used to quantify mutation frequency of target single nucleotide substitutions,
 275 namely M:D3N (G26529A), S:R346T (G22599C), S:N460K (T22942G) and S:K4444T
 276 (A22893C). Two probes with different Nanopixel barcodes were used for each target mutation,
 277 one targeting the wild-type sequence and the other the mutated sequence. For Hyperplex PCR,
 278 the mutation frequency is calculated as the ratio of counts (RCPs) for the mutant sequence to
 279 those of the wild-type sequence. The plot showing expected vs observed mutant frequency was
 280 obtained using synthetic PCR amplicons (ssDNA) spiked in solution. The plot showing
 281 correlation between hpPCR and NGS mutation frequency was obtained by testing wastewater
 282 samples (w42/2022 to w48/2022) targeting M:D3, S:N460, S:R346 and S:K444. **B-** Early
 283 detection of mutations and variants of concern using Hyperplex PCR vs NGS. S:F486P, S:F456L
 284 and S:Q52H were characteristic of variants XBB 1.5, EG.5 and EG.5.1 when measurements were
 285 initiated. Tested mutations for BA.2.86 include S:483del, S:F157S/R158G, Orf1:A7842G and
 286 S:69-70del. NGS data refers to the same mutations targeted by Hyperplex PCR. The y axis refers
 287 to different collection sites as follows: 1- Göteborg, 2- Helsingborg, 3- Malmö, 4- Örebro, 5-
 288 Stockholm-Käppala, 6- Umeå, 7- Uppsala, 8- Västerås. The heatmap below each chart refers to

289 the fraction of clinical samples collected in Sweden found to be positive for each of the target
290 mutations under analysis.

291

292 **3. Conclusions**

293 Despite the mounting evidence of the potential of WBE for surveillance of present and
294 future pathogen outbreaks and pandemics, the field is still in its infancy with regards to
295 method and output standardization. The current typical WBE approach is schematized in
296 Figure 4 according to alternative 1 where surveillance typically focuses on quantitative
297 monitoring of a limited number of pathogens of interest using target specific qPCR or
298 dPCR. For the surveillance of variants and mutations, this is complemented either by
299 NGS, which is typically successful only in case of sufficiently high titers, or alternatively,
300 by individual mutation specific qPCR or dPCR assays. In this approach there is often a
301 dilemma between reagent and labor cost-effectiveness and necessary performance
302 including the optimization of qPCR or dPCR assays for novel targets, which often
303 culminates with researchers circling back to costly NGS, particularly when several point
304 mutations, become targets of interest as is the case for most SARS-CoV-2 viral variants.
305 Alternatively, Hyperplex PCR is herein demonstrated as a powerful tool enabling
306 affordable quantitative and qualitative high-frequency multi-pathogen wastewater
307 monitoring, deployable in virtually any research lab. As demonstrated here has a
308 performance competitive with state-of-the-art NGS methods, the possibility of rapidly
309 including new probes on-demand and a simple workflow with results from extracted RNA
310 within one workday. Towards enabling a next-generation single-method surveillance
311 approach, Hyperplex PCR thus successfully fills the bioanalytical method gap between
312 qPCR/dPCR and NGS, upgrading the current WBE analytical toolbox by providing: (1)
313 High multiplexity per sample with single nucleotide specificity, (2) NGS-grade mutation
314 frequency quantification with a good correlation ($r = 0.88$) extremely high linearity ($R^2 >$
315 0.99), (3) 4-weeks+ early detection of variants of concern demonstrated vs sequencing,
316 (4) Panel customization with new probes within 2 weeks without panel re-optimization.
317 Based on the results of the long-term study reported herein, the authors believe that
318 hpPCR, particularly upon maximization of multiplexity towards the theoretical limits of
319 100+ target sequences and complemented with open data platforms for rapid probe design
320 and panel customization has the potential to become a gold-standard for sustainable and
321 standardized WBE.



322

323 **Figure 4:** Current approach typically used for WBE during and after the SARS-CoV-2 pandemic
324 (Alt.1) resorting to qPCR, dPCR and NGS for high-frequency monitoring and proposed
325 alternative approach (Alt. 2) using only hpPCR. The delay until actionable results includes the
326 time to design and validate new primers/probes for emerging mutations/variants in the case of
327 qPCR/dPCR and/or the time to select the ideal method among qPCR, dPCR and NGS to strike an
328 adequate balance between sensitivity and specificity of mutation identification within a certain
329 setting.

330

331 4. Methods

332 4.1. Wastewater sample collection and extraction

333 For each site, we collected weekly samples of untreated wastewater integrated over a
334 single day (24 hours) using flow-compensated samplers. All measurements represent only
335 one day except for Uppsala, where daily samples were combined flow-proportionally into
336 one composite sample representing one week. The processing of samples followed the
337 protocols outlined in Isaksson et al. [27] involving the concentration and extraction of
338 viral genomic material using the Maxwell RSC Enviro TNA kit (Promega). All nucleic
339 acid extracts were stored at -80 °C until further processing.

340

341

342 **4.2. qPCR quantification of SARS-CoV-2 and PMMoV**

343 The absolute quantification of SARS-CoV-2 genome copy numbers followed the
344 methodology outlined in Isaksson et al. [27]. Until w31/2023 quantification was
345 performed using the SARS-CoV-2 specific N1 assay [28] while from w32/2023 the Flu
346 SC2 Multiplex Assay (CDC) was utilized. To account for variations in population size
347 and wastewater flow, the SARS-CoV-2 genome copy numbers were normalized to pepper
348 mild mottle virus (PMMoV) copy numbers. PMMoV quantification followed a modified
349 version of the assay described by Zhang et al [29]

350

351 **4.3. Next generation sequencing (NGS)**

352 The generated total nucleic acid (TNA) extracts were sequenced either on Thermo
353 Fisher's Ion Torrent System (w40/2022-w21/2023 and w35-36/2023), or on Illumina
354 (w22-34/2023 and w37-52/2023).

355

356 **4.3.1. Ion torrent sequencing**

357 The sequencing libraries for Ion Torrent were prepared from the extracted total nucleic
358 acids were prepared using the Ion AmpliSeq™ SARS-COV-2 Insight Research Assay
359 (Thermo Fisher Scientific) and the SuperScript™ VILO™ cDNA Synthesis Kit (Thermo
360 Fisher), following the manufacturer's protocols "Reverse transcribe RNA with the
361 SuperScript™ VILO™ cDNA Synthesis Kit" (Thermo Fisher) and "Prepare libraries on
362 the Ion Chef™ Instrument" (Thermo Fisher) with the Ion Chef System. Sequencing was
363 conducted on the Ion S5 XL System (Thermo Fisher) by multiplexing using Torrent Suite
364 Software version 5.16.1 as per to the manufacturer's instructions (Thermo Fisher). The
365 generated sequence data were filtered, aligned to the manufacturer's references
366 (Ion_AmpliSeq_SARS-CoV-2-Insight_Reference), and used to generate mutation
367 frequency tables for variant detection using the manufacturer's analysis pipeline in
368 Torrent Suite 5.16 (Thermo Fisher, # MAN0017972 Rev B.0, Ch 12). Library
369 preparation, Ion Torrent sequencing, and sequence analyses were carried out at the
370 National Genomics Infrastructure (NGI) at Science for Life Laboratory, Uppsala,
371 Sweden.

372

373 **4.3.1. Illumina sequencing**

374 For the Illumina sequencing, DNase treatment (DNase I, Amplification Grade,
375 Invitrogen) was performed to reduce unspecific amplification before library preparation

376 by the COVIDSeq Assay kit (Illumina). Samples from weeks 22, 23, 33, and 34/2023
377 were amplified using the Artic V4.1 NCOV-2019 Panel primers (IDT DNA), while the
378 remaining samples sequenced by Illumina technology were amplified using the Artic
379 V5.3.2 NCOV-2019 Panel primers (IDT DNA). The resulting libraries were sequenced
380 either on the Illumina MiSeq platform using the MiSeq Reagent Kit v3 2 x 76 (150-cycle)
381 (Illumina) (w22-34/2023 and w40/2023), or the Illumina NextSeq 550 platform using the
382 NextSeq Reagent Kit 500/550 High Output Kit v2 2 x 74 (150-cycle) (Illumina) (w37-
383 39/2023 and w41-52/2023). The generated sequence data were processed and used to
384 generate mutation frequency tables for variant detection using variant quantification in
385 sewage pipeline designed for robustness (VaQuERo.v2) [2]. Library preparation,
386 Illumina sequencing, and sequence analyses were carried at the Swedish University of
387 Agriculture Sciences (SLU).

388

389 **4.4. Single-reaction 18-plex mutation detection with Hyperplex PCR**

390 The Hyperplex PCR reaction comprises 3 main steps, (1) PCR amplification, PLP ligation
391 and RCA; (2) RCP capture and probing with Nanopixel probes; (3) Imaging of the surface
392 using a fluorescence microscope. The amplification, capture and labelling protocol was
393 performed according to instructions of a custom Hyperplex PCR kit assembled by
394 APLEX Bio including the PCR primers and PLP sequences listed in Table 1.

395

396 **4.4.1. Probe design, PCR amplification, PLP ligation and RCA**

397 To maximize PCR efficiency, all PCR primers according to Table S1 were designed to
398 generate amplicons with less than 250 bp and having within 5% CV of melting
399 temperature averaging 63 °C. Reference sequences for each target mutation and/or variant
400 were obtained via the European COVID-19 Data Portal and the GISAID initiative [30].
401 Depending on sequence availability at the date probes were included in the panel, 15 to
402 200 sequences from Swedish patients were aligned and used for primer and probe design.
403 RT-PCR amplification was performed by combining 2 µL of extracted nucleic acids with
404 8 µL a master mix containing all relevant primers for the targets under analysis. Final
405 primer concentrations were between 50 and 150 nM for the forward primers and 67 to
406 300 nM for the reverse primers according to Tables S2, S3, S4 and S5. The mix was then
407 subjected to the following temperatures using a thermal cycler: 25°C for 2 min, 50°C for
408 15 min, 95°C for 2 min, followed by 40 cycles of [95°C for 3 sec, 60°C for 1 min]. After
409 PCR, the amplicons were diluted with 190 µL DNase/RNase-free water water and 0.5 µL

410 of the diluted mixture were combined with 19.5 μL of Ligation mixture in a separate PCR
411 tube, comprising the mix of PLPs (50 pM to 1 nM each final concentration), ligation
412 buffer and hpPCR Ligase. For PLP ligation, the mixture was placed in the thermocycler
413 and subjected to 95 $^{\circ}\text{C}$ for 20 s and 60 $^{\circ}\text{C}$ for 30 min. 10 μL of RCA master mix containing
414 hpPCR polymerase were then added to the 20 μL ligation mix and subjected to an
415 additional 2 hours at 37 $^{\circ}\text{C}$, followed by enzyme inactivation at 60 $^{\circ}\text{C}$ for 20 min. All
416 temperature cycling and incubation steps were performed in a Bio-Rad T100 thermal
417 cyclor with default temperature ramp conditions.

418

419 **4.4.2. RCP capture and probing with Nanopixels**

420 After RCA, 2.5 μL of the RCP solution was combined with 50 μL of capture buffer
421 containing an RCP reference. The RCP reference serves as an internal control to
422 normalize the capture efficiency of RCPs on the surface. 40 μL of this mix were then
423 transferred into the wells of the slide frame mounted on the capture slide provided in the
424 kit, followed by incubation for 5 min at room temperature. Afterwards, 100 μL of absolute
425 EtOH were added to each well on top of the capture solution and all contents were
426 subsequently discarded. The wells were then washed twice with wash buffer, followed
427 by 50 μL of blocker buffer which was left to incubate 5 min at room temperature. The
428 solution was then removed and 40 μL of labelling master mix containing the probes were
429 added. After 60 min incubation at 37 $^{\circ}\text{C}$ using an incubator oven (Mettler BE200), the
430 solution was removed, each well washed four times with 50 μL wash buffer, the slide
431 frame was disassembled and finally mounted using antifade solution (SlowFade™
432 Diamond Antifade Mountant, Thermo Fisher Scientific).

433

434 **4.4.3. Fluorescence microscopy imaging**

435 The microscope used for imaging was a Zeiss Axio Imager 2 equipped with a Hamamatsu
436 Orca Fusion sCMOS camera, a Colibri 7 solid-state light source, a 20x Plan-Apochromat
437 20x/0.8 M27 objective and the following emission filter sets from CHROMA: 525/50 BP,
438 605/52 BP, 690/50 BP, 785/25 BP. Image acquisition was performed with 9 tiles per
439 sample. Analysis of the raw czi files was performed using a proprietary software tool
440 from APLEX Bio including the following general functions: (1) image cropping and
441 background subtraction, (2) channel alignment, (3) segmentation, (4) spot processing and
442 extraction, (5) Nanopixel decoding algorithm and (6) output of counts per color code
443 normalized to an internal reference. For all target mutations, the signal was corrected

444 (cutoff baseline) using an internal control sample containing 1.000 copies/ μ L of wild-
445 type SARS-CoV-2 IVT RNA (Twist Bioscience Viral Control 2, Wuhan-Hu-1,
446 MN908947.3). All signals above the detection threshold are higher than the average
447 signal of the control plus $3.29 \times SD$ ($n=4$).

448

449 **Acknowledgements**

450 The data handling was enabled by resources provided by the National Academic
451 Infrastructure for Supercomputing in Sweden (NAISS), partially funded by the Swedish
452 Research Council through grant agreement no. 2022-06725. Ion Torrent sequencing was
453 performed by the SNP&SEQ Technology Platform in Uppsala. The facility is part of the
454 National Genomics Infrastructure (NGI) Sweden and Science for Life Laboratory. The
455 SNP&SEQ Platform is also supported by the Swedish Research Council and the Knut and
456 Alice Wallenberg Foundation. This work was funded by governmental grants provided
457 to the Public Health Agency of Sweden for assignment S2022/04841. We further
458 acknowledge the Public Health Agency of Sweden for contributions to padlock probe
459 target design. U.N. and R.S. are co-inventors of the hpPCR methodology according to
460 patent application WO/2021/206614. U.N. holds shares in Aplex Bio AB. Other authors
461 declare no competing financial interests.

462

463 **References**

- 464 [1] H. R. Safford, K. Shapiro, and H. N. Bischel, ‘Wastewater analysis can be a
465 powerful public health tool—if it’s done sensibly’, *Proceedings of the National
466 Academy of Sciences of the United States of America*, vol. 119, no. 6. National
467 Academy of Sciences, Feb. 08, 2022. doi: 10.1073/pnas.2119600119.
- 468 [2] F. Amman *et al.*, ‘Viral variant-resolved wastewater surveillance of SARS-CoV-2
469 at national scale’, *Nat Biotechnol*, vol. 40, no. 12, pp. 1814–1822, Dec. 2022, doi:
470 10.1038/s41587-022-01387-y.
- 471 [3] X. Li *et al.*, ‘Wastewater-based epidemiology predicts COVID-19-induced weekly
472 new hospital admissions in over 150 USA counties’, *Nat Commun*, vol. 14, no. 1,
473 Dec. 2023, doi: 10.1038/s41467-023-40305-x.
- 474 [4] M. J. Wade, J. T. Bunce, S. Petterson, C. Ferguson, N. C. del Campo, and E.
475 Gaddis, ‘Editorial: Wastewater-based epidemiology at the frontier of global public
476 health’, *J Water Health*, Feb. 2023, doi: 10.2166/wh.2023.001.
- 477 [5] K. Farkas *et al.*, ‘Wastewater-based monitoring of SARS-CoV-2 at UK airports
478 and its potential role in international public health surveillance’, *PLOS Global*

- 479 *Public Health*, vol. 3, no. 1, p. e0001346, Jan. 2023, doi:
480 10.1371/journal.pgph.0001346.
- 481 [6] M. M. Shafer *et al.*, ‘Tracing the origin of SARS-CoV-2 omicron-like spike
482 sequences detected in an urban sewershed: a targeted, longitudinal surveillance
483 study of a cryptic wastewater lineage’, *Lancet Microbe*, Mar. 2024, doi:
484 10.1016/S2666-5247(23)00372-5.
- 485 [7] S. E. Philo *et al.*, ‘A comparison of SARS-CoV-2 wastewater concentration
486 methods for environmental surveillance’, *Science of the Total Environment*, vol.
487 760, Mar. 2021, doi: 10.1016/j.scitotenv.2020.144215.
- 488 [8] M. Perez-Zabaleta *et al.*, ‘Long-term SARS-CoV-2 surveillance in the wastewater
489 of Stockholm: What lessons can be learned from the Swedish perspective?’,
490 *Science of the Total Environment*, vol. 858, Feb. 2023, doi:
491 10.1016/j.scitotenv.2022.160023.
- 492 [9] K. Farkas *et al.*, ‘Rapid Assessment of SARS-CoV-2 Variant-Associated
493 Mutations in Wastewater Using Real-Time RT-PCR’, *Microbiol Spectr*, vol. 11,
494 no. 1, Feb. 2023, doi: 10.1128/spectrum.03177-22.
- 495 [10] W. Ahmed *et al.*, ‘Comparison of RT-qPCR and RT-dPCR Platforms for the Trace
496 Detection of SARS-CoV-2 RNA in Wastewater’, *ACS ES and T Water*, vol. 2, no.
497 11, pp. 1871–1880, Nov. 2022, doi: 10.1021/acsestwater.1c00387.
- 498 [11] J. Ding, X. Xu, Y. Deng, X. Zheng, and T. Zhang, ‘Comparison of RT-ddPCR and
499 RT-qPCR platforms for SARS-CoV-2 detection: Implications for future outbreaks
500 of infectious diseases’, *Environ Int*, vol. 183, Jan. 2024, doi:
501 10.1016/j.envint.2024.108438.
- 502 [12] Y. Liu *et al.*, ‘Multiplex Assays Enable Simultaneous Detection and Identification
503 of SARS-CoV-2 Variants of Concern in Clinical and Wastewater Samples’, *ACS*
504 *Measurement Science Au*, vol. 3, no. 4, pp. 258–268, Aug. 2023, doi:
505 10.1021/acsmesuresciau.3c00005.
- 506 [13] B. Malla, O. Thakali, S. Shrestha, T. Segawa, M. Kitajima, and E. Haramoto,
507 ‘Application of a high-throughput quantitative PCR system for simultaneous
508 monitoring of SARS-CoV-2 variants and other pathogenic viruses in wastewater’,
509 *Science of the Total Environment*, vol. 853, Dec. 2022, doi:
510 10.1016/j.scitotenv.2022.158659.
- 511 [14] M. Fuzzen *et al.*, ‘An improved method for determining frequency of multiple
512 variants of SARS-CoV-2 in wastewater using qPCR assays’, *Science of the Total*
513 *Environment*, vol. 881, Jul. 2023, doi: 10.1016/j.scitotenv.2023.163292.
- 514 [15] J. Ding, X. Xu, Y. Deng, X. Zheng, and T. Zhang, ‘Circulation of SARS-CoV-2
515 Omicron sub-lineages revealed by multiplex genotyping RT-qPCR assays for
516 sewage surveillance’, *Science of the Total Environment*, vol. 904, Dec. 2023, doi:
517 10.1016/j.scitotenv.2023.166300.
- 518 [16] L. Heijnen, G. Elsinga, M. de Graaf, R. Molenkamp, M. P. G. Koopmans, and G.
519 Medema, ‘Droplet digital RT-PCR to detect SARS-CoV-2 signature mutations of

- 520 variants of concern in wastewater’, *Science of the Total Environment*, vol. 799,
521 Dec. 2021, doi: 10.1016/j.scitotenv.2021.149456.
- 522 [17] E. G. Lou *et al.*, ‘Direct comparison of RT-ddPCR and targeted amplicon
523 sequencing for SARS-CoV-2 mutation monitoring in wastewater’, *Science of the
524 Total Environment*, vol. 833, Aug. 2022, doi: 10.1016/j.scitotenv.2022.155059.
- 525 [18] J. Ho, C. Stange, R. Suhrborg, C. Wurzbacher, J. E. Drewes, and A. Tiehm,
526 ‘SARS-CoV-2 wastewater surveillance in Germany: Long-term RT-digital droplet
527 PCR monitoring, suitability of primer/probe combinations and biomarker
528 stability’, *Water Res*, vol. 210, Feb. 2022, doi: 10.1016/j.watres.2021.117977.
- 529 [19] S. Wurtzer *et al.*, ‘From Alpha to Omicron BA.2: New digital RT-PCR approach
530 and challenges for SARS-CoV-2 VOC monitoring and normalization of variant
531 dynamics in wastewater’, *Science of the Total Environment*, vol. 848, Nov. 2022,
532 doi: 10.1016/j.scitotenv.2022.157740.
- 533 [20] M. Kuroiwa *et al.*, ‘Targeted amplicon sequencing of wastewater samples for
534 detecting SARS-CoV-2 variants with high sensitivity and resolution’, *Science of
535 the Total Environment*, vol. 893, Oct. 2023, doi: 10.1016/j.scitotenv.2023.164766.
- 536 [21] G. La Rosa *et al.*, ‘Wastewater surveillance of SARS-CoV-2 variants in October–
537 November 2022 in Italy: detection of XBB.1, BA.2.75 and rapid spread of the
538 BQ.1 lineage’, *Science of the Total Environment*, vol. 873, May 2023, doi:
539 10.1016/j.scitotenv.2023.162339.
- 540 [22] F. Cancela *et al.*, ‘Wastewater surveillance of SARS-CoV-2 genomic populations
541 on a country-wide scale through targeted sequencing’, *PLoS One*, vol. 18, no. 4
542 April, Apr. 2023, doi: 10.1371/journal.pone.0284483.
- 543 [23] R. R. G. Soares, N. Madaboosi, and M. Nilsson, ‘Rolling Circle Amplification in
544 Integrated Microsystems: An Uncut Gem toward Massively Multiplexed Pathogen
545 Diagnostics and Genotyping’, *Acc Chem Res*, vol. 54, no. 21, pp. 3979–3990, Nov.
546 2021, doi: 10.1021/acs.accounts.1c00438.
- 547 [24] U. NASEEM and R. R. G. SOARES, ‘A METHOD FOR MULTIPLEXED
548 DETECTION OF A PLURALITY OF TARGET BIOMOLECULES’,
549 WO/2021/206614, Oct. 14, 2021
- 550 [25] G. J. S. Lohman *et al.*, ‘A high-throughput assay for the comprehensive profiling
551 of DNA ligase fidelity’, *Nucleic Acids Res*, vol. 44, no. 2, p. e14, Jan. 2016, doi:
552 10.1093/nar/gkv898.
- 553 [26] C. Chen *et al.*, ‘CoV-Spectrum: Analysis of globally shared SARS-CoV-2 data to
554 identify and characterize new variants’, *Bioinformatics*, vol. 38, no. 6, pp. 1735–
555 1737, Mar. 2022, doi: 10.1093/bioinformatics/btab856.
- 556 [27] F. Isaksson, L. Lundy, A. Hedström, A. J. Székely, and N. Mohamed, ‘Evaluating
557 the Use of Alternative Normalization Approaches on SARS-CoV-2
558 Concentrations in Wastewater: Experiences from Two Catchments in Northern
559 Sweden’, *Environments - MDPI*, vol. 9, no. 3, Mar. 2022, doi:
560 10.3390/environments9030039.

- 561 [28] C. B. F. Vogels *et al.*, ‘Analytical sensitivity and efficiency comparisons of SARS-
562 CoV-2 RT–qPCR primer–probe sets’, *Nat Microbiol*, vol. 5, no. 10, pp. 1299–
563 1305, Oct. 2020, doi: 10.1038/s41564-020-0761-6.
- 564 [29] T. Zhang *et al.*, ‘RNA viral community in human feces: Prevalence of plant
565 pathogenic viruses’, *PLoS Biol*, vol. 4, no. 1, pp. 0108–0118, Jan. 2006, doi:
566 10.1371/journal.pbio.0040003.
- 567 [30] S. Elbe and G. Buckland-Merrett, ‘Data, disease and diplomacy: GISAID’s
568 innovative contribution to global health’, *Global Challenges*, vol. 1, no. 1, pp. 33–
569 46, Jan. 2017, doi: 10.1002/gch2.1018.
- 570